Supplement of

Emissions of Organic Compounds from Western US Wildfires and their Near Fire Transformations

Yutong Liang et al.

Correspondence to: Yutong Liang (yutong.liang@berkeley.edu)

This Supplement contains:

1. Improved calibration and quantification method for particle phase compounds – Page S2
2. Estimation of saturation vapor pressure of particle phase compounds – Page S2-S3
3. Calculation of adjusted EF – Page S3
4. Supplementary figures and tables – Page S4-S15
5. Supplementary references Page S16-S17

1. Improved calibration and quantification method for particle phase compounds

In our previous work, most compounds were quantified by normalizing them to their nearest internal standard in the GC×GC space, and then applying the calibration curve of those compounds themselves or surrogate external standards. We manually picked external standards to quantify analyte compounds of interest. The assignment of both external standard and internal standard are improved in this work. First, we calculated two parameters, i.e., 2D distance on the GC×GC space and spectral cosine similarity to aid our decision on which (surrogate) external standard should we use for quantifying the compound of interest. The cosine similarity (CS) is calculated by:

$$CS = \frac{\overrightarrow{MS_1} \cdot \overrightarrow{MS_2}}{\left|\overrightarrow{MS_1}\right|\left|\overrightarrow{MS_2}\right|} \tag{S1}$$

where $\overrightarrow{MS_1}$ and $\overrightarrow{MS_2}$ are the mass spectra vector of the compound being quantified, and the mass spectra vector of the standard, respectively (Isaacman-VanWertz et al., 2020; Stein, 1994). Two identical mass spectral will have a CS = 1, while two orthogonal mass spectra will have a CS = 0.

Some internal standards co-elute with other compounds in the chromatogram. Cutting such co-eluting blobs can cause large uncertainties for quantification. Also, the purposes of internal standards are to correct for the drift of system response, and loss of analytes during sample preparation and derivatization. We strive to use an internal standard compound similar to the compound being calibrated to achieve the highest accuracy. Therefore, in this work, we compared the R^2 of the calibration curves of standard compounds based on normalization to the nearest internal standard, and the R^2 based on normalization to the nearest deuterated alkane standard. The internal standard producing the higher R^2 was chosen. This method improved the average R^2 of standard calibration curves by 0.11.

2. Estimation of saturation vapor pressures of particle phase compounds

In our previous work, we estimated the solid state saturation vapor pressure of compounds (Liang et al., 2021). However, there is evidence that organic compounds in the complex mixture have liquid-like properties (Koponen et al., 2007; Riipinen et al., 2007). Also, partitioning models and the volatility basis set (VBS) model use the subcooled liquid vapor pressure as inputs (Booth et al., 2010; Donahue et al., 2011). Therefore, in this work, we estimated the subcooled liquid pressures of compounds instead. The subcooled liquid vapor pressures of compounds were estimated by three methods. First, for compounds identified with formula and structure (n = 148), we used the SIMPOL model (Pankow and Asher, 2008) via the GECKO-A platform (http://geckoa.lisa.u-pec.fr), the PEACh package (Isaacman-Vanwertz and Aumont, 2021) and/or manual calculation to get their subcooled liquid vapor pressures at 298 K. We noticed that the SIMPOL model may substantially overestimate the vapor pressure of nitro-aromatic compounds than experimental data and predictions from other models. For instance, the saturation vapor pressure of 4-nitrophenol is predicted to be 32 Pa at 298K, while the experimental data and the predictions from other

models give pressures on the order of 10^{-3} Pa (Bannan et al., 2017; Wania et al., 2017). Therefore, we used the MPBPWIN component (modified Grain method) in EPA's EPI Suite (US EPA, 2012) to estimate the subcooled saturation vapor pressures of these nitro-aromatic compounds. For compounds with confirmed formula but unconfirmed structure (n = 28), we estimated the saturation vapor pressures using the method by Li et al. (2016), also via the PEACh package. For the rest 64 compounds without confirmed formulae, similar to our previous work, we trained a regression model (with 5-fold cross validation) using the MATLAB (version 2021b) Regression Learner to predict their saturation vapor pressure v_P. Compound class, first column retention index, and second column retention time were used as the inputs, and $\log_{10}(v_P)$ was the output. The training dataset includes all the standard compounds (with their vapor pressures calculated by SIMPOL). The root-mean-square error (RMSE) and R^2 of the model are 0.93 and 0.86, respectively.

3. Calculation of adjusted EF

While laboratory burns offer some advantages over field burns, conditions may be sufficiently different to warrant adjustments of laboratory-derived emission factors (EFs) to better represent field fires. Specifically, in laboratory experiments modified combustion efficiency (MCE) is typically higher than in wildfires. Previous studies have described and applied methods for adjusting laboratory-derived EFs (e.g., Christian et al. (2003), Yokelson et al. (2008), Selimovic et al. (2018)). Most commonly, laboratory EFs for individual compounds or classes of compounds are plotted as a function of MCE and the data are fit using linear regression; the slope and intercept of the linear fit allows calculation of a field-adjusted EF based on the field-derived MCE. This method requires having enough data points for each compound/class of compounds to obtain a robust linear regression. As shown in Stockwell et al. (2015) and Permar et al. (2021), the slope and intercept are dependent on the compound/compound class and thus global fits are not appropriate. Here, a modified approach was applied in which the EF ratio of the compound of interest to CO was averaged between FIREX laboratory and field measurements:

$$\mathrm{EF}_{adjusted} = \frac{1}{2}\left(\frac{\mathrm{EF}_{i,lab}}{\mathrm{EF}_{CO,lab}} + \frac{\mathrm{EF}_{i,field}}{\mathrm{EF}_{CO,field}}\right) \times \mathrm{EF}_{CO,field} \quad \text{(S1)}$$

where $\mathrm{EF}_{\mathrm{adjusted}}$ is the adjusted emission factor, EF_i is the emission of compound i. Averaging the laboratory and field $\mathrm{EF}_{\mathrm{compound}}/\mathrm{EF}_{\mathrm{CO}}$ accounts for the combustion-type-specific information from both laboratory and field studies, while multiplying by $\mathrm{EF}_{\mathrm{CO,field}}$ removes bias from the higher overall MCE (higher flaming/smoldering ratio) in the laboratory studies than in the field. In this work, the field EFs were calculated by averaging across the Arizona and Nethker samples.

4. Supplementary figures and tables

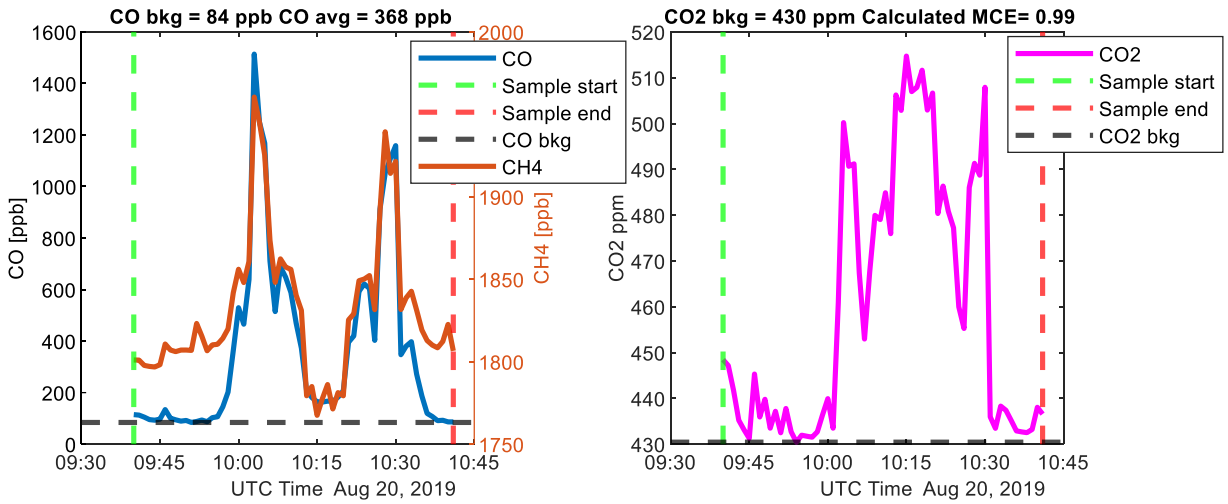

Figure S1: Example of an hourly sample affected by CO_2 unknown source. The CO_2 peak around 10:15 was from unknown source because CO or CH4 were not elevated simultaneously with CO_2. It caused a very high hourly integrated "MCE" that cannot represent the combustion efficiency of the two major plumes at 10:03 and 10:30.

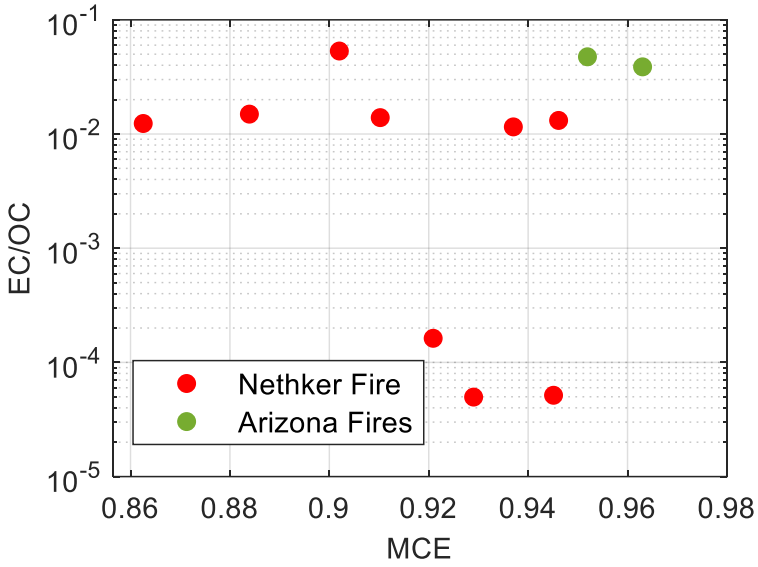

Figure S2: EC/OC ratio vs MCE. No clear trend is observed.

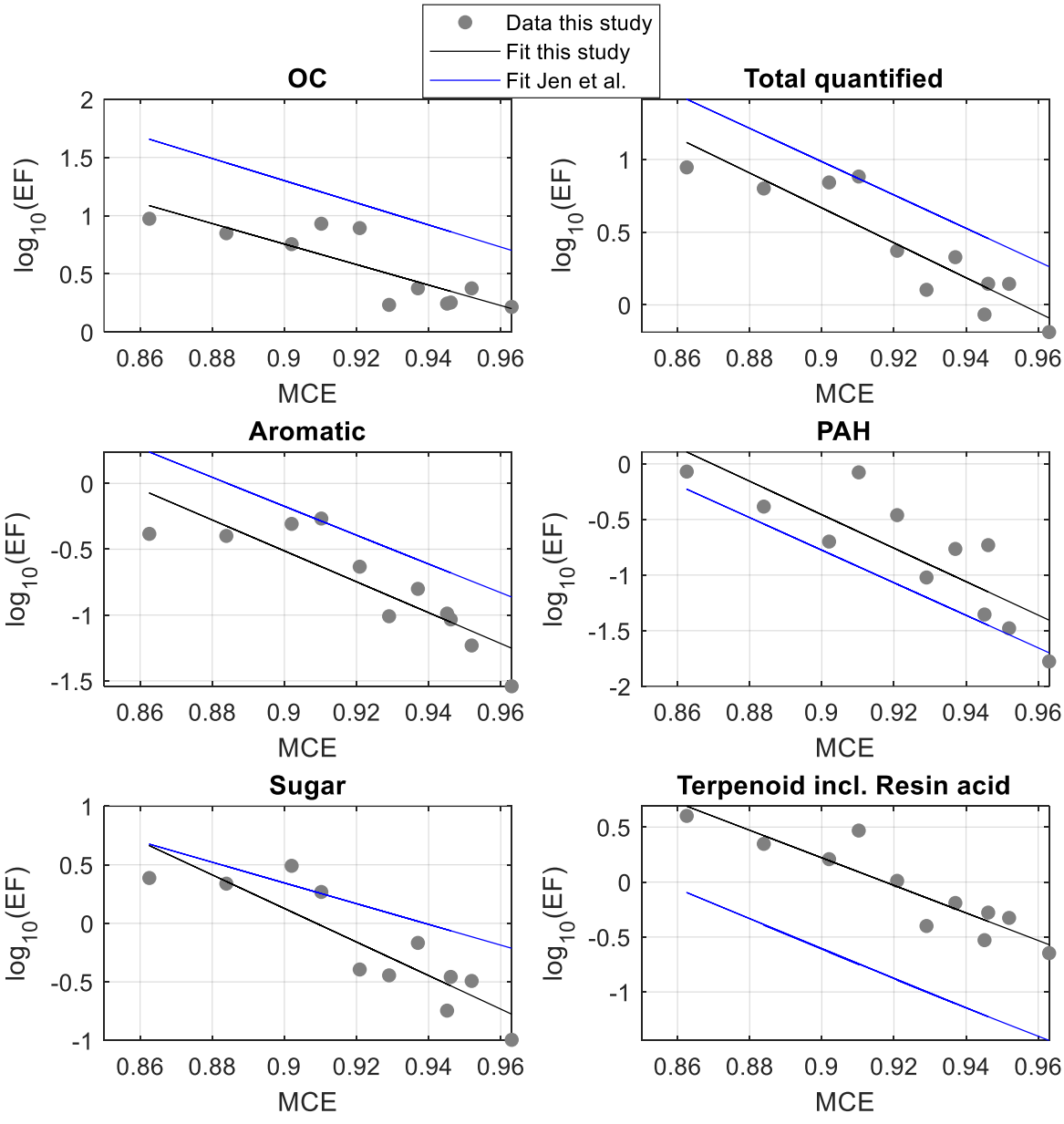

Figure S3: Comparison of emission factors of OC and average summed emission factors of compounds in this study and in Jen et al. (2019).

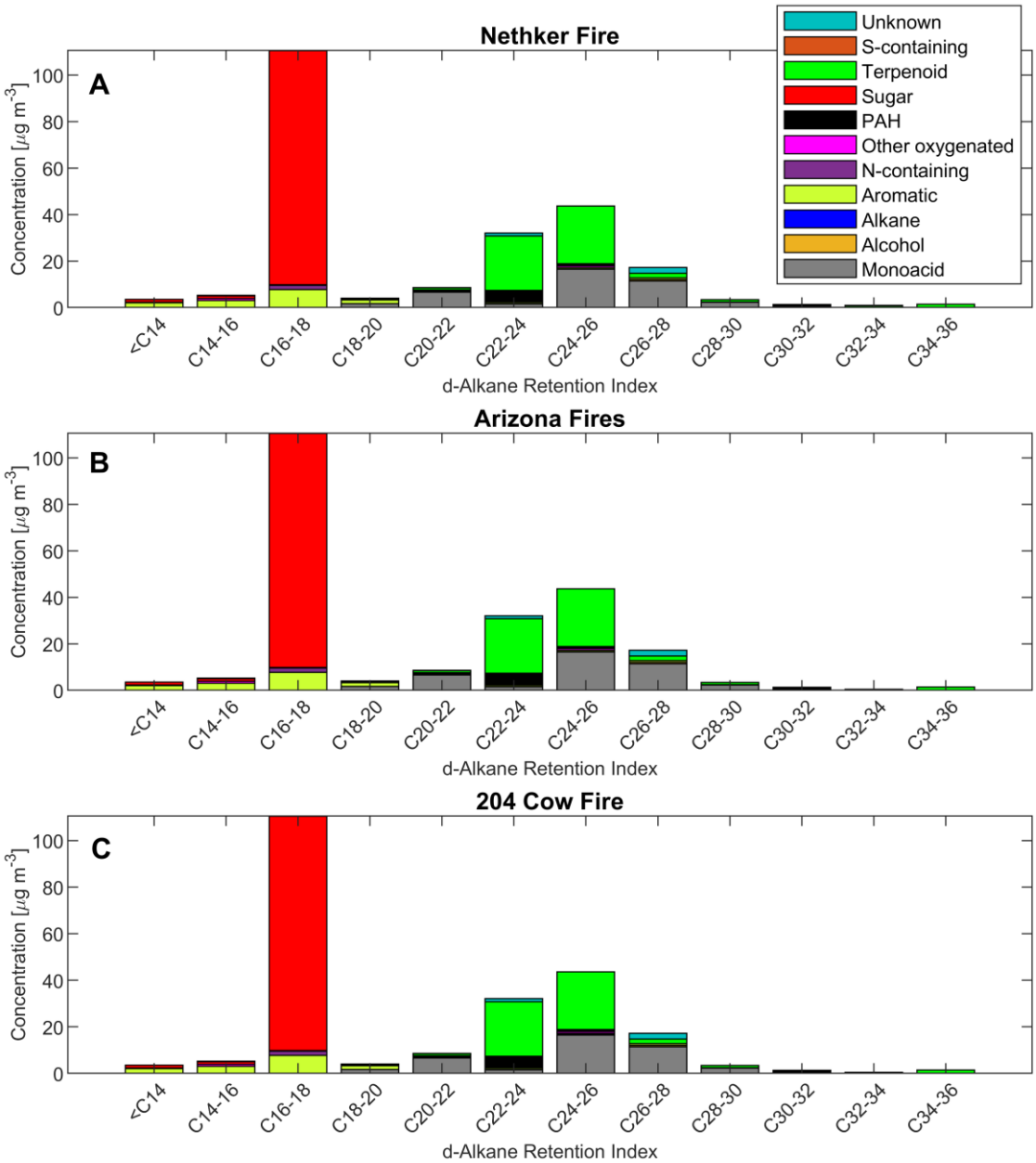

Figure S4: Mass distribution of speciated compounds in different rentention index bins. Retention index is linearly related to retention time. (**A**) is for the most heavily loaded sample collected near the Nethker Fire (OC = 352 μg m^{-3}); (**B**) is for the most heavily loaded sample collected near the Arizona Ikes and Castle Fires (OC = 138 μg m^{-3}); (**C**) is for the most heavily loaded sample collected near the 204 Cow Fire (OC = 260 μg m^{-3}). N = 1 in each plot.

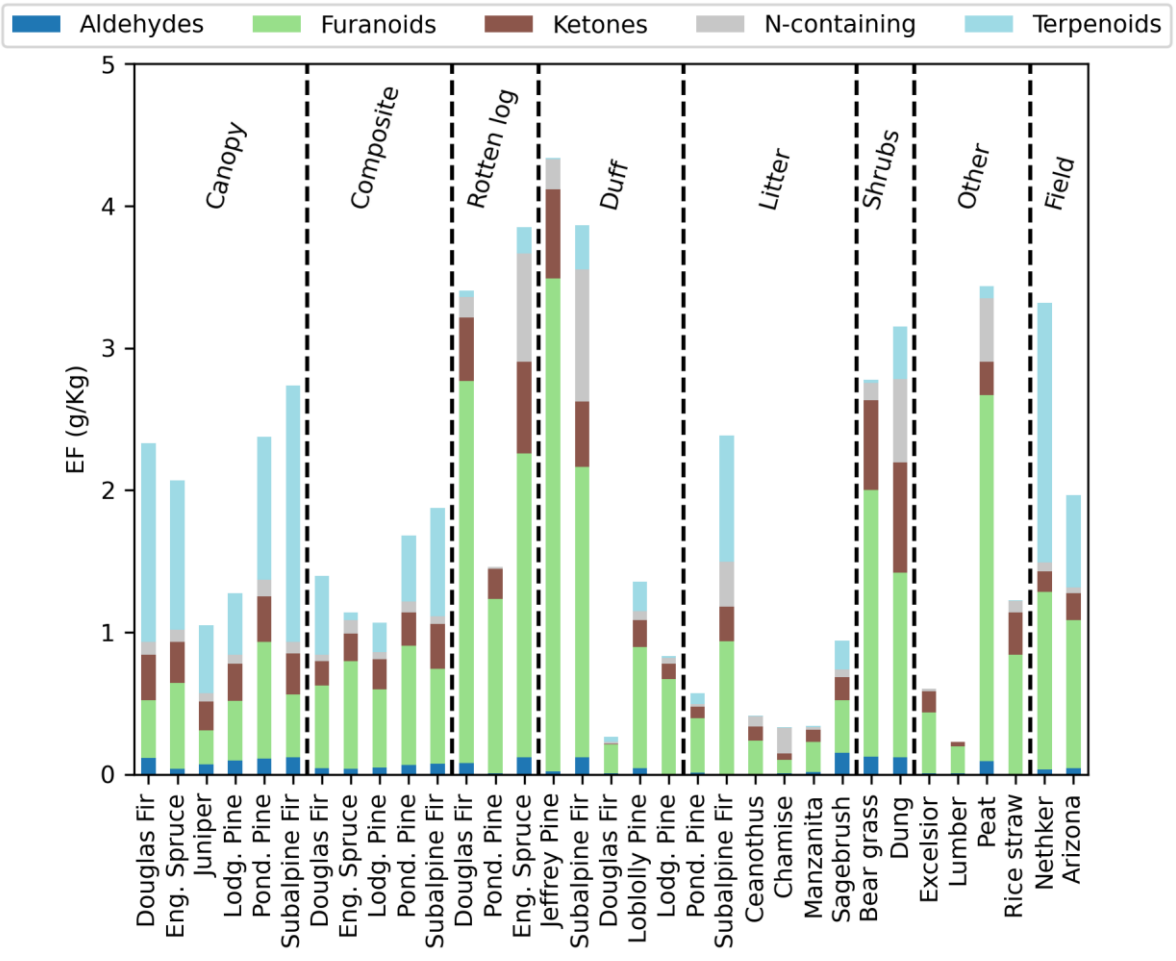

Figure S5: Average summed emission factors of 5 groups of VOCs (terpenoid, ketones, aldehydes, N-containing and furanoids) from this study and from burning each fuel in the Fire Lab 2016 study.

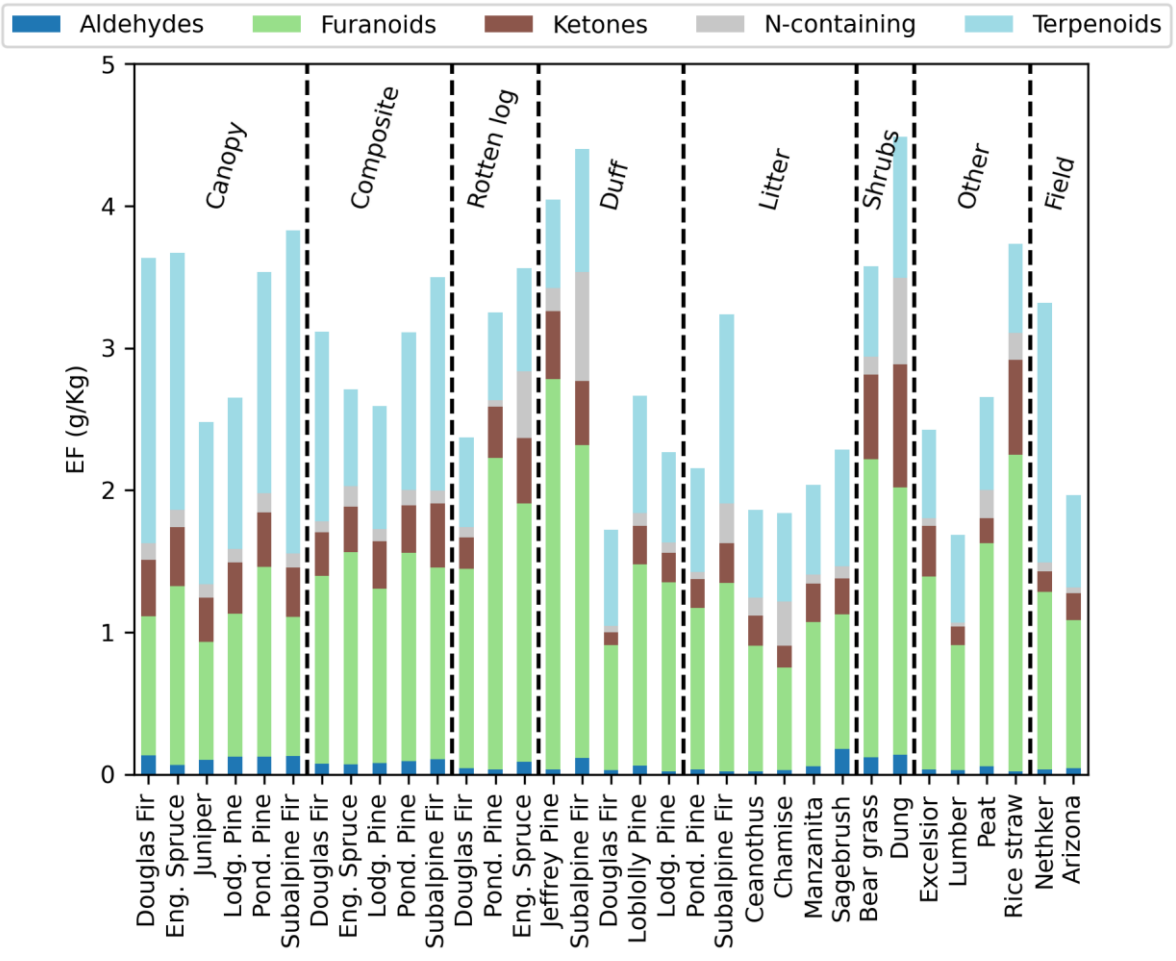

Figure S6: Average summed **adjusted** emission factors of 5 groups of VOCs (terpenoid, ketones, aldehydes, N-containing and furanoids) from this study and from burning each fuel in the Fire Lab 2016 study.

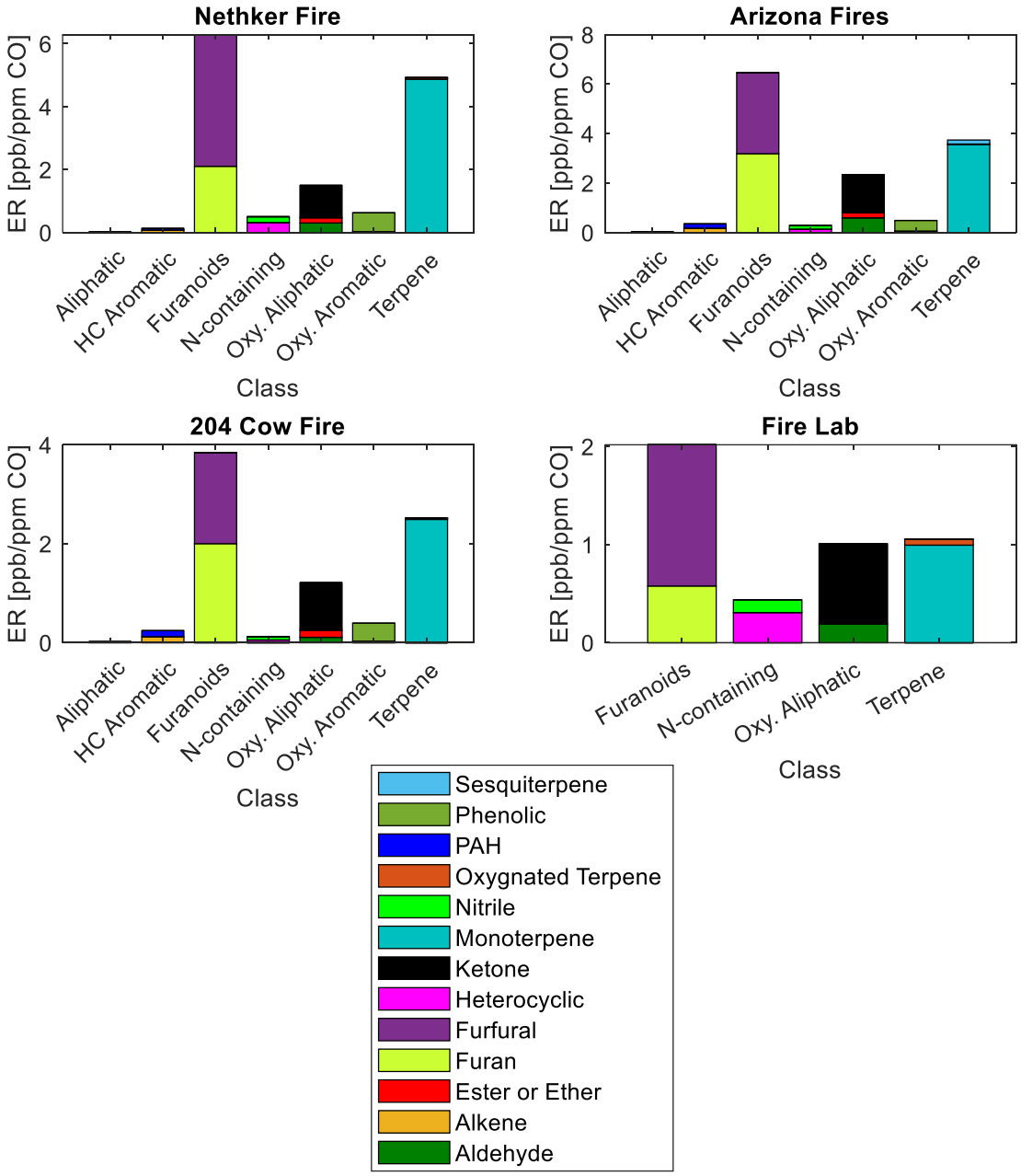

Figure S7: Average emission ratios of observed VOCs in Nethker Fire (N = 2), Arizona Fires (N = 3), and 204 Cow Fire (N = 3), grouped by chemical classification. Results from the Fire Lab study are the average of all fuels. Only furanoids, nitrogen-containing compounds, oxygenated aliphatic compounds and terpenes were quantified in the Fire Lab study.

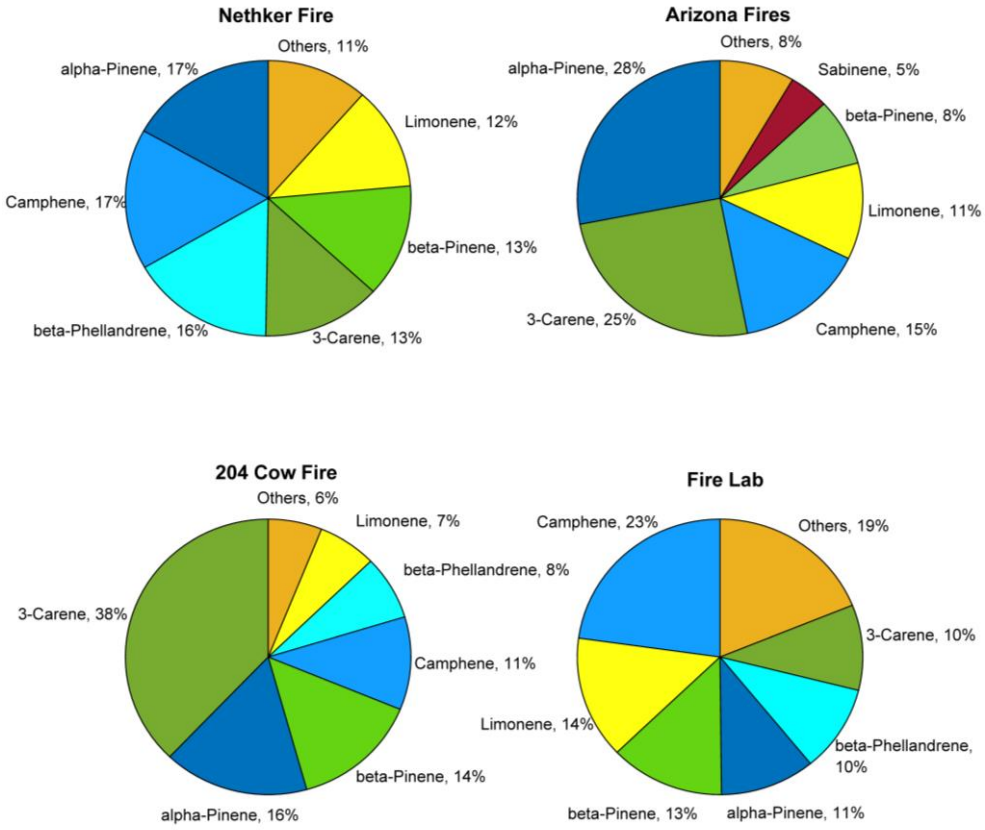

Figure S8: The fraction of gas phase terpenoids emission ratio (with respect to CO) attributed to the top 6 observed terpenoids and other tepenoids.

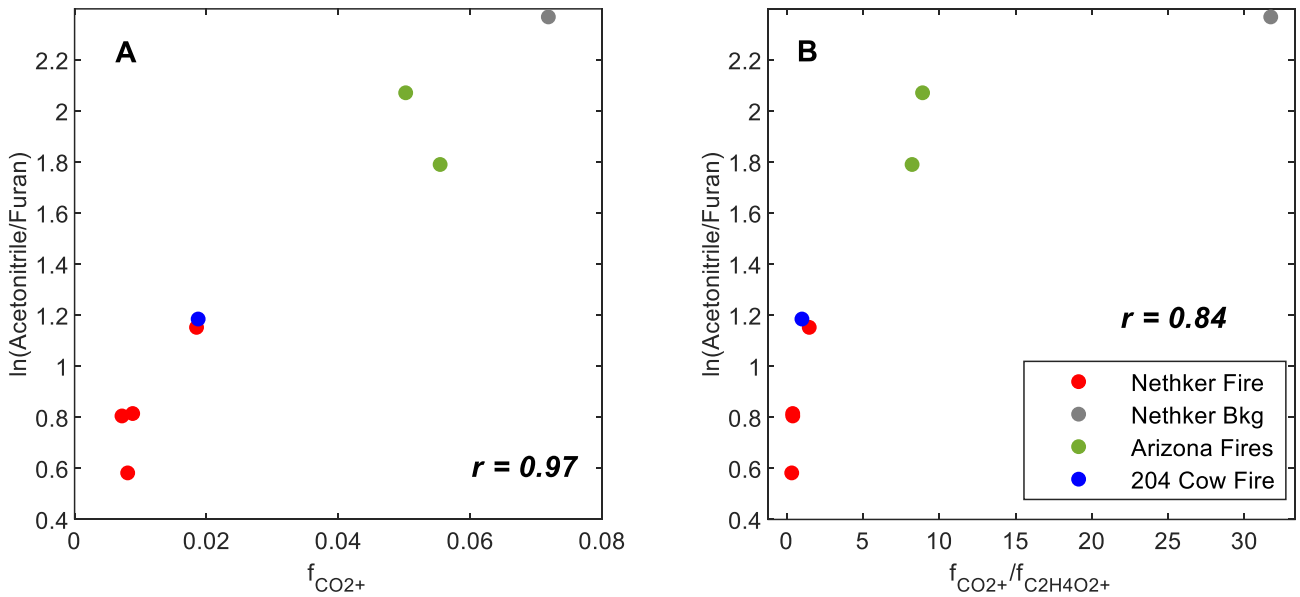

Figure S9: The ln(Acetonitrile/Furan) ratio vs **A.** f_{CO2+} and **B.** $f_{CO2+}/f_{C2H4O2+}$ from SP-AMS. They have strong positive correlations.

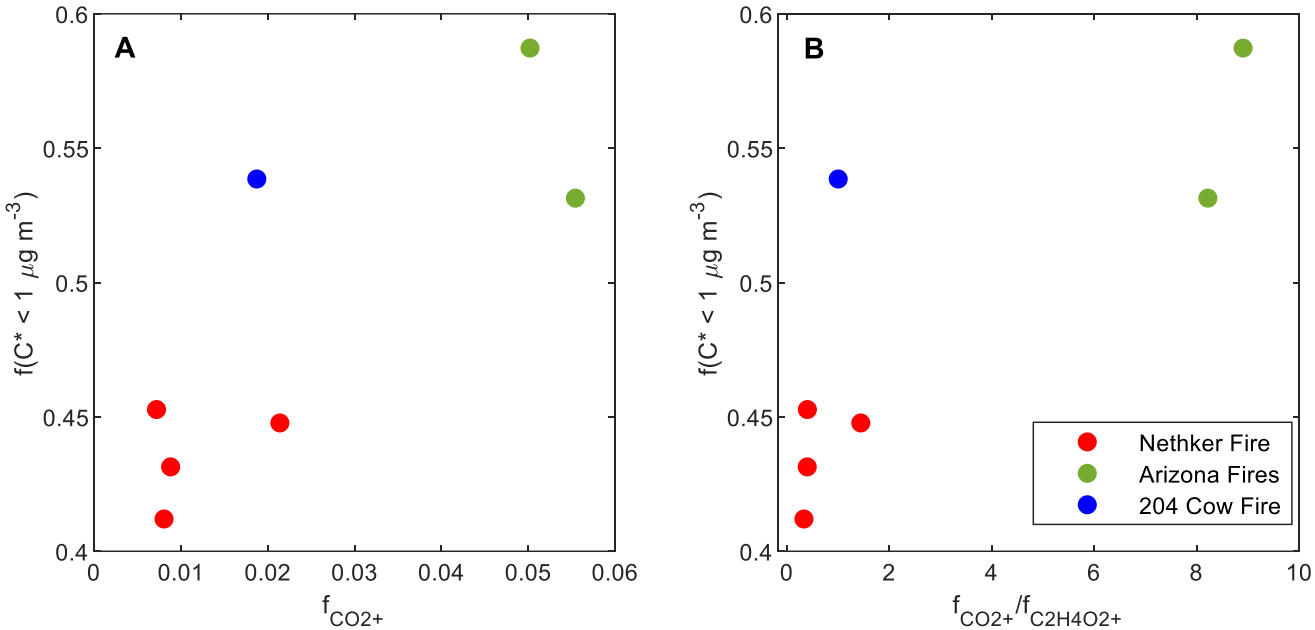

Figure S10: Mass fraction of summed concentration of observed particle phase compounds with C* < 1 μg m^{-3} in total quantified OA, as a function of **A.** f_{CO2+} and **B.** $f_{CO2+}/f_{C2H4O2+}$.

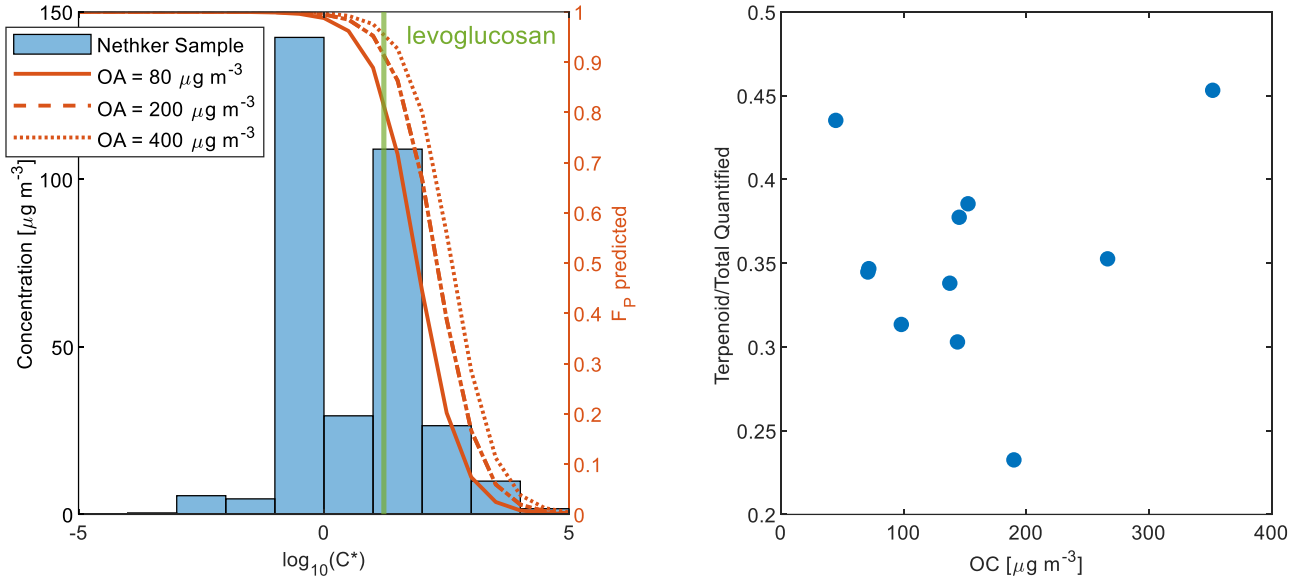

Figure S11: Left: Mass distribution of speciated compounds in different effective saturation concentration bins for the most heavily loaded sample collected near the Nethker Fire, and the predicted particle phase fraction (F_p) as a function of effective saturation concentration. Vertical line shows the $\log_{10}(C^*)$ of levoglucosan, the dominant compound in that bin. Right: Mass fraction of terpenoids (including resin acids) in total quantified OA vs. OC.

Table S1 Standards for calibration, their linear retention indices based on *n*-alkanes and their secondary retention time.

Compound	LRI *n*-alkane	RT2 (s)	Compound	LRI *n*-alkane	RT2 (s)
(-)verbenone	1198	1.86	**C32 alkane**	3200	0.53
(+)borneol	1216	0.53	**C33 alkane**	3300	0.55
1,2-acenaphthylenedione	1876	2.16	**C34 alkane**	3400	0.56
1,2-benzanthracene	2472	1.15	**C35 alkane**	3500	0.60
16-hydroxyhexadecanoic acid	2385	0.61	**C36 alkane**	3600	0.64
2,4-dinitrophenol	1752	2.24	**C6 diacid**	1502	0.90
2-ketoglutaric acid	1603	0.70	**C8 acid**	1257	0.67
2-methylthreitol	1530	0.48	**C9 acid**	1357	0.64
2-pentadecanone	1698	0.83	**catechol**	1309	0.62
3,3-dimethylglutaric acid	1505	0.81	**cholestane**	2865	0.72
3,5-dimethoxyphenol	1501	0.79	**cholesterol**	3150	0.72
3-decanol	1284	0.44	**chrysene**	2483	1.15
3-guaiacylpropanol	1525	0.59	**coniferyl aldehyde**	1840	1.36
3-hydroxy-3-methylglutaric acid	1597	0.72	**D-(+)-mannose**	1792	0.52
3-methyl-5-nitrocatechol	1830	1.35	**dehydroabietic acid**	2387	0.71
3-octadecanone	1996	0.73	**dibenz(a,h)anthracene**	3217	1.32
4,4-dimethoxy-benzophenone	2251	1.29	**dibenzofuran**	1525	0.86
4-hydroxybenzoic acid	1624	0.81	**dodecanedioic acid**	2083	0.79
4-methyl-5-nitrocatechol	1773	1.26	**eicosanol**	2347	0.47
4-methylcatechol	1383	0.58	**ergosterol**	3235	0.70
4-nitrocatechol	1740	1.41	**erythritol**	1505	0.48
5-(hydroxymethyl)furfural	1309	1.25	**fluoranthene**	2077	1.09
5-nitrovanillin	1836	1.91	**fluorene**	1592	0.88
9H-fluoren-9-one	1746	1.24	**gamma-dodecalactone**	1679	1.72
abietic acid	2423	0.72	**glucose**	1900	0.55
acetosyringone	1761	1.16	**glyceric acid**	1324	0.60
acetovanillone	1615	1.16	**Hexadecane, 2,6,10,14-tetramethyl-**	1806	0.46
alpha amyrin	3413	0.90	**hexadecanol**	1956	0.46
anthracene	1804	0.98	**hydroquinone**	1397	0.67
anthraquinone	1981	1.31	**indeno(1,2,3-cd)pyrene**	3205	1.40
azelaic acid	1791	0.84	**isoeugenol**	1565	0.68
benzo(a)pyrene	2885	1.28	**isopimaric acid**	2341	0.75
benzo(b)fluoranthene	2793	1.25	**levoglucosan**	1699	0.76
benzo(g,h,i)perylene	3276	1.39	**linoleic acid**	2206	0.59
benzo(k)fluoranthene	2801	1.25	**malic acid**	1485	0.76
benzoic acid	1241	0.78	**maltol**	1279	1.04

benzophenone	1634	1.06	**3-methyl-1,2,3-butanetricarboxylic acid**	1746	0.86
beta-sitosterol	3343	0.73	**monopalmitin**	2581	0.62
bornyl acetate	1282	0.94	**octadecanal**	2021	0.73
C10 acid	1455	0.63	**octadecanol**	2152	0.45
C11 acid	1552	0.61	**oleic acid**	2212	0.59
C12 acid	1651	0.62	**palmitoleic acid**	2021	0.59
C13 acid	1746	0.60	**p-anisic acid**	1519	0.88
C14 acid	1846	0.60	**pentadecane, 2,6,10,14-tetramethyl-**	1705	0.45
C15 alkane (normal alkane, same below)	1500	0.43	**phenanthrene**	1792	0.98
C15 acid	1944	0.61	**phthalamide**	1566	1.04
C16 alkane	1600	0.41	**phthalic acid**	1686	1.01
C16 acid	2043	0.61	**pinic acid**	1663	0.87
C17 alkane	1700	0.41	**pinic acid isomer**	1670	0.87
C17 acid	2139	0.59	**pinonic acid**	1524	1.33
C18 alkane	1800	0.43	**protocatechuic acid**	1814	0.71
C18 acid	2240	0.60	**pyrogallol**	1535	0.53
C19 alkane	1900	0.45	**pyrogallol isomer**	1595	0.59
C20 alkane	2000	0.46	**quinoline**	1239	0.98
C20 acid	2437	0.59	**resorcinol**	1377	0.66
C21 alkane	2100	0.45	**retene**	2225	0.93
C22 alkane	2200	0.45	**sinapaldehyde**	2001	1.41
C22 acid	2635	0.61	**stigmasterol**	3283	0.72
C23 alkane	2300	0.46	**syringaldehyde**	1699	1.22
C23 acid	2734	0.60	**syringic acid**	1892	0.77
C24 alkane	2400	0.47	**syringol**	1396	0.74
C24 acid	2834	0.60	**terpinen-4-ol**	1166	0.68
C25 alkane	2500	0.47	**tetradecane-1,14-dioic acid**	2277	0.76
C26 alkane	2600	0.49	**threitol**	1497	0.47
C26 acid	3031	0.61	**tricarballylic acid**	1727	0.90
C27 alkane	2700	0.51	**tridecanal**	1512	0.81
C28 alkane	2800	0.50	**tyrosol**	1566	0.57
C28 acid	3230	0.61	**vaccenic acid**	2219	0.59
C29 alkane	2900	0.51	**vanillic acid**	1757	0.78
C30 alkane	3000	0.52	**vanillin**	1532	1.24
C31 alkane	3100	0.52	**xanthone**	1872	1.23

5. Supplementary references

Bannan, T. J., Booth, A. M., Jones, B. T., O'Meara, S., Barley, M. H., Riipinen, I., Percival, C. J. and Topping, D.: Measured Saturation Vapor Pressures of Phenolic and Nitro-aromatic Compounds, Environ. Sci. Technol., 51(7), 3922–3928, doi:10.1021/acs.est.6b06364, 2017.

Booth, A. M., Barley, M. H., Topping, D. O., McFiggans, G., Garforth, A. and Percival, C. J.: Solid state and sub-cooled liquid vapour pressures of substituted dicarboxylic acids using Knudsen Effusion Mass Spectrometry (KEMS) and Differential Scanning Calorimetry, Atmos. Chem. Phys, 10, 4879–4892, doi:10.5194/acp-10-4879-2010, 2010.

Christian, T. J., Kleiss, B., Yokelson, R. J., Holzinger, R., Crutzen, P. J., Hao, W. M., Saharjo, B. H. and Ward, D. E.: Comprehensive laboratory measurements of biomass-burning emissions: 1. Emissions from Indonesian, African, and other fuels, J. Geophys. Res. Atmos., 108(23), 4719, doi:10.1029/2003jd003704, 2003.

Donahue, N. M., Epstein, S. A., Pandis, S. N. and Robinson, A. L.: A two-dimensional volatility basis set: 1. organic-aerosol mixing thermodynamics, Atmos. Chem. Phys., 11(7), 3303–3318, doi:10.5194/acp-11-3303-2011, 2011.

Isaacman-Vanwertz, G. and Aumont, B.: Impact of organic molecular structure on the estimation of atmospherically relevant physicochemical parameters, Atmos. Chem. Phys, 21, 6541–6563, doi:10.5194/acp-21-6541-2021, 2021.

Isaacman-VanWertz, G., Lu, X., Weiner, E., Smiley, E. and Widdowson, M.: Characterization of Hydrocarbon Groups in Complex Mixtures Using Gas Chromatography with Unit-Mass Resolution Electron Ionization Mass Spectrometry, Anal. Chem., 92(18), 12481–12488, doi:10.1021/acs.analchem.0c02308, 2020.

Jen, C. N., Hatch, L. E., Selimovic, V., Yokelson, R. J., Weber, R., Fernandez, A. E., Kreisberg, N. M., Barsanti, K. C. and Goldstein, A. H.: Speciated and total emission factors of particulate organics from burning western US wildland fuels and their dependence on combustion efficiency, Atmos. Chem. Phys., 19(2), 1013–1026, doi:10.5194/acp-19-1013-2019, 2019.

Koponen, I. K., Riipinen, I., Hienola, A., Kulmala, M. and Bilde, M.: Thermodynamic properties of malonic, succinic, and glutaric acids: Evaporation rates and saturation vapor pressures, Environ. Sci. Technol., 41(11), 3926–3933, doi:10.1021/es0611240, 2007.

Li, Y., Pöschl, U. and Shiraiwa, M.: Molecular corridors and parameterizations of volatility in the chemical evolution of organic aerosols, Atmos. Chem. Phys., 16(5), 3327–3344, doi:10.5194/acp-16-3327-2016, 2016.

Liang, Y., Jen, C. N., Weber, R. J., Misztal, P. K. and Goldstein, A. H.: Chemical composition of PM2.5 in October 2017 Northern California wildfire plumes, Atmos. Chem. Phys., 21(7), 5719–5737, doi:10.5194/acp-21-5719-2021, 2021.

Pankow, J. F. and Asher, W. E.: SIMPOL.1: A simple group contribution method for predicting vapor pressures and enthalpies of vaporization of multifunctional organic compounds, Atmos. Chem. Phys., 8(10), 2773–2796, doi:10.5194/acp-8-2773-2008, 2008.

Permar, W., Wang, Q., Selimovic, V., Wielgasz, C., Yokelson, R. J., Hornbrook, R. S., Hills, A. J., Apel, E. C., Ku, I. T., Zhou, Y., Sive, B. C., Sullivan, A. P., Collett, J. L., Campos, T. L., Palm, B. B., Peng, Q., Thornton, J. A., Garofalo, L. A., Farmer, D. K., Kreidenweis, S. M., Levin, E. J. T., DeMott, P. J., Flocke, F., Fischer, E. V. and Hu, L.: Emissions of Trace

Organic Gases From Western U.S. Wildfires Based on WE-CAN Aircraft Measurements, J. Geophys. Res. Atmos., 126(11), doi:10.1029/2020JD033838, 2021.

Riipinen, I., Koponen, I. K., Frank, G. P., Hyvärinen, A. P., Vanhanen, J., Lihavainen, H., Lehtinen, K. E. J., Bilde, M. and Kulmala, M.: Adipic and malonic acid aqueous solutions: Surface tensions and saturation vapor pressures, J. Phys. Chem. A, 111(50), 12995–13002, doi:10.1021/jp073731v, 2007.

Selimovic, V., Yokelson, R. J., Warneke, C., Roberts, J. M., De Gouw, J., Reardon, J. and Griffith, D. W. T.: Aerosol optical properties and trace gas emissions by PAX and OP-FTIR for laboratory-simulated western US wildfires during FIREX, Atmos. Chem. Phys., 18(4), 2929–2948, doi:10.5194/acp-18-2929-2018, 2018.

Stein, S. E.: Estimating probabilities of correct identification from results of mass spectral library searches, J. Am. Soc. Mass Spectrom., 5(4), 316–323, doi:10.1016/1044-0305(94)85022-4, 1994.

Stockwell, C. E., Veres, P. R., Williams, J. and Yokelson, R. J.: Characterization of biomass burning emissions from cooking fires, peat, crop residue, and other fuels with high-resolution proton-transfer-reaction time-of-flight mass spectrometry, Atmos. Chem. Phys., 15(2), 845–865, doi:10.5194/acp-15-845-2015, 2015.

US EPA: Estimation Programs Interface Suite™ for Microsoft® Windows, United States Environ. Prot. Agency,Washington, DC, USA, 2012.

Wania, F., Awonaike, B. and Goss, K. U.: Comment on “measured Saturation Vapor Pressures of Phenolic and Nitro-Aromatic Compounds,” Environ. Sci. Technol., 51(13), 7742–7743, doi:10.1021/acs.est.7b02079, 2017.

Yokelson, R. J., Christian, T. J., Karl, T. G. and Guenther, A.: The tropical forest and fire emissions experiment: Laboratory fire measurements and synthesis of campaign data, Atmos. Chem. Phys., 8(16), 4497, doi:10.5194/acp-8-4497-2008, 2008.